



An Analysis of Parameters for the Johnson-Cook Strength Model for 2-in-Thick Rolled Homogeneous Armor

by Hubert W. Meyer, Jr. and David S. Kleponis

ARL-TR-2528

June 2001

Approved for public release; distribution is unlimited.

20010717 111

The findings in this report are not to be construed as an official Department of the Army position unless so designated by other authorized documents.

Citation of manufacturer's or trade names does not constitute an official endorsement or approval of the use thereof.

Destroy this report when it is no longer needed. Do not return it to the originator.

Army Research Laboratory

Aberdeen Proving Ground, MD 21005-5066

ARL-TR-2528

June 2001

An Analysis of Parameters for the Johnson-Cook Strength Model for 2-in-Thick Rolled Homogeneous Armor

Hubert W. Meyer, Jr. and David S. Kleponis
Weapons and Materials Research Directorate, ARL

Abstract

Yield strength obtained from quasi-static strength data for rolled homogeneous armor (RHA) was combined with dynamic strength data for 2-in (51-mm) RHA to generate Johnson-Cook parameters for 2-in RHA. One parameter was fixed based on the quasi-static strength data, and a least-squares method was used to fit the others individually. The fit was tested with CTH by simulating the penetration of stacks of 2.5-in-thick (63.5-mm) RHA plates (the closest available experimental data). Parameter analysis and comparison of the simulations to experiment substantiated the approach.

Acknowledgments

The authors would like to acknowledge Shuh Rong Chen for providing the raw data (in digital form) that was used in this report.

This work was supported in part by a grant of high-performance computing time from the Department of Defense High Performance Computing Center at Aberdeen Proving Ground, MD.

INTENTIONALLY LEFT BLANK.

Table of Contents

	<u>Page</u>
Acknowledgments	iii
List of Figures.....	vii
List of Tables	vii
1. Introduction.....	1
2. Dynamic Data	3
3. Quasi-Static Data	4
4. Fitting the Parameters	5
4.1 Parameter A	5
4.2 Parameters B and n	6
4.3 Parameter C.....	8
4.4 Parameter m	10
5. Numerical Simulations	13
5.1 Setup	13
5.2 Results.....	14
5.3 Discussion	17
6. Conclusion	19
7. References.....	21
Distribution List.....	23
Report Documentation Page	25

INTENTIONALLY LEFT BLANK.

List of Figures

<u>Figure</u>	<u>Page</u>
1. RHA Hardness Variations Specified by MIL-A-12560H	1
2. Dynamic Strength of 2-in RHA	4
3. Quasi-Static Yield Strength of RHA.....	6
4. Simulation Setup.....	14
5. Nose and Tail Tracer Histories for the 1,616 m/s, Set 2 Case	16
6. Set 2: 1,616-m/s Penetration Plot	18

List of Tables

<u>Table</u>	<u>Page</u>
1. Dynamic Strength Data for 2-in RHA	4
2. Quasi-Static Yield Strength of RHA.....	5
3. Strain-Rate Dependence of Room-Temperature Data	9
4. Quadratic Fit of the Temperature Data	12
5. RHA Parameter Sets Evaluated	15
6. RHA Penetrations in Millimeters for the Parameter Sets Evaluated	15

INTENTIONALLY LEFT BLANK.

1. Introduction

Class 1 rolled homogeneous armor (RHA), designed for maximum penetration resistance, is available in thicknesses from 1/4 in (6.35 mm) up to 6 in (152.4 mm). Military specification MIL-A-12560H (U.S. Department of Defense 1991) allows a wide variation in hardness over the range of available thicknesses as well as within each thickness group (Figure 1). Since hardness is an indicator of several material strength properties, a significant variation in material properties exists over the range of thicknesses of available RHA and to a lesser extent, within each thickness group.

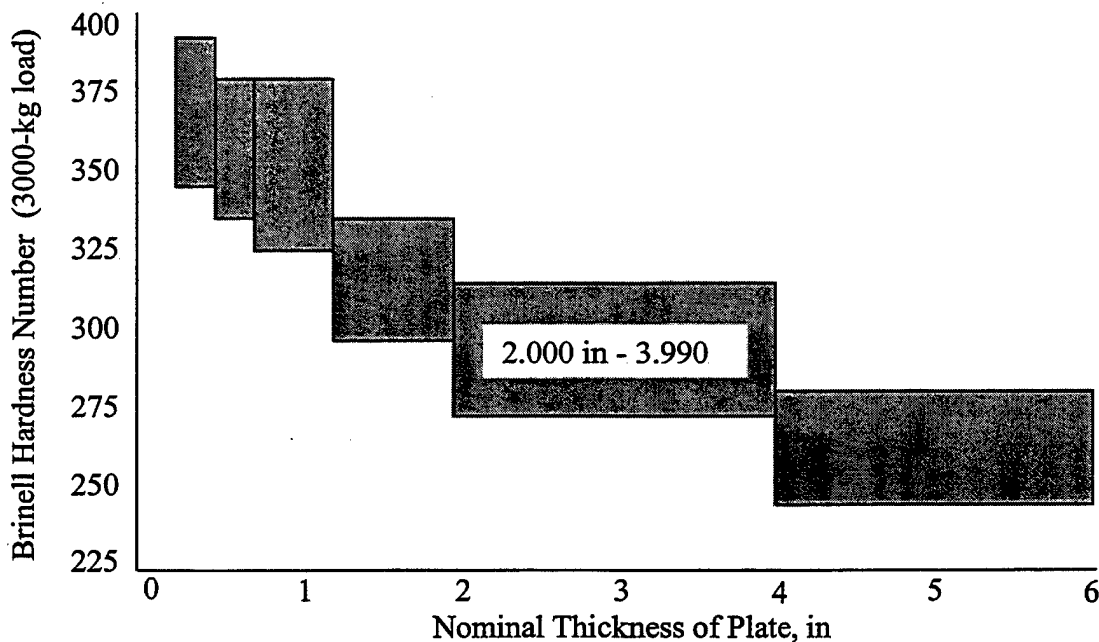


Figure 1. RHA Hardness Variations Specified by MIL-A-12560H.

To properly model the ballistic performance of RHA, consideration must be given to these property variations. The wide variation in material properties across the spectrum of available thicknesses suggests that each thickness should be separately evaluated to obtain valid strength parameters. Further complications exist (e.g., manufacturing lots and through-the-thickness hardness variations). However, these complexities are avoided in the present work by assuming

that the variations in properties for a particular thickness, as allowed by the thickness group, are negligible. That is, for an RHA plate that conforms to MIL-A-12560H, specifying its thickness is sufficient in identifying its properties.

The shock physics code CTH (McGlaun et al. 1990) is used at the U.S. Army Research Laboratory (ARL) to model ballistic impact and penetration experiments. The Johnson-Cook strength model (Johnson and Cook 1983) is one of several strength models available in CTH. It is an empirical model that computes material flow stress as a function of strain (work) hardening, strain-rate hardening, and thermal softening. The Johnson-Cook model takes the following form:

$$Y = A \left(1 + \frac{B}{A} \epsilon^n \right) (1 + C \ln \dot{\epsilon}^*) (1 - T^{*m}), \quad (1)$$

where A, B, C, m, and n are constants, ϵ is the equivalent plastic strain, $\dot{\epsilon}^*$ is the strain rate nondimensionalized by the reference strain rate of 1/s, and T^* is the nondimensional temperature. Parameter A, the initial ($\epsilon \approx 0$) yield strength of the material at a plastic strain rate of $\dot{\epsilon} = 1/s$ and room temperature (298 K), is modified by a strain-hardening factor (containing parameters B and n), a strain-rate-hardening factor (containing parameter C), and a thermal-softening factor (containing parameter m).

T^* is defined by

$$T^* = \frac{T - T_r}{T_m - T_r}, \quad (2)$$

where T_r is room temperature and T_m is the melting temperature of the material, 1,783 K for RHA. Equation (2) is the form used in CTH and is valid for $T_r \leq T \leq T_m$, the region of interest in most ballistic applications.

CTH originally contained a single set of parameters that had been typically used in simulations for any thickness of RHA. These parameters were taken from one of two data fits for RHA presented in Gray et al. (1994). Both of these fits (which will be discussed) were determined using 2-in-thick RHA that conformed to MIL-A-12560H. The fits resulted in overprediction of the quasi-static yield strength (A in equation [1]). Their approach to optimization was to consider all parameters simultaneously. This approach to fitting the data resulted in a model for the RHA that underpredicted the depth of penetration of several experiments; this is discussed in more detail later. In the present work, Johnson-Cook parameters are developed for that particular batch of 2-in-thick RHA. The approach taken here is to fix the value of A based on the quasi-static test data. An optimum fit to the data for each of the remaining parameters is then found individually, as suggested by Johnson and Cook (1983).

2. Dynamic Data

Gray et al. (1994) generated compressive stress-strain data for a variety of metals over a range of temperatures and strain rates using the split-Hopkinson pressure bar. The digital data consisted of the results of dynamic tests of 2-in-thick RHA. At room temperature, tests were conducted at four strain rates (0.001; 0.1; 3,500; and 7,000/s). At elevated temperatures (473 and 673 K) tests were conducted at a strain rate of 3,000/s. Strains were recorded from near zero up to about 0.20.

To expedite processing time and utilize all of the available data, the digital data was not used directly to obtain the Johnson-Cook parameters, rather it was fit to analytical functions that were suitable to the software available for use during this study. The fits of the six data sets are shown graphically in Figure 2 and algebraically in Table 1. The functions in Table 1 are fits to the RHA strength data from Gray et al. (1994) and are used to determine the Johnson-Cook parameters in the following analyses. For clarity, yield strength predicted by the Johnson-Cook model is denoted by Y (in GPa), whereas y (in GPa) represents the data fits.

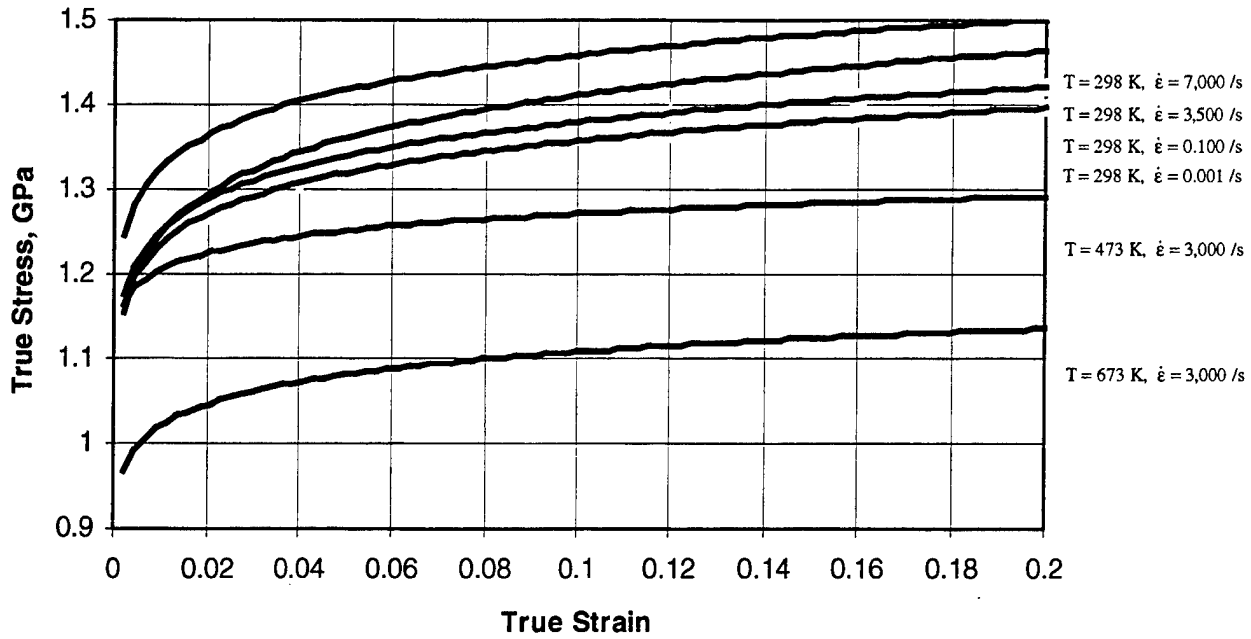


Figure 2. Dynamic Strength of 2-in RHA.

Table 1. Dynamic Strength Data for 2-in RHA

Temperature (K)	Strain Rate (/s)	Function	Equation No.
298	0.001	$y = 1.4905\epsilon^{0.0407}$	(3a)
298	0.100	$y = 1.5206\epsilon^{0.0423}$	(3b)
298	3,500	$y = 1.5935\epsilon^{0.0529}$	(3c)
298	7,000	$y = 1.6048\epsilon^{0.0415}$	(3d)
473	3,000	$y = 1.3410\epsilon^{0.0231}$	(3e)
673	3,000	$y = 1.2029\epsilon^{0.0357}$	(3f)

(3)

3. Quasi-Static Data

Benck (1976) determined several properties for three thicknesses of RHA. He measured the quasi-static tensile yield strength in the three principal plate directions (in the rolling direction, across the rolling direction, and through the thickness) at a strain rate of 0.0003/s. For present purposes, these values were averaged to obtain a representative isotropic value. The

compressive yield strength of the material is then assumed to be equal to the tensile yield strength; this is only approximately true for RHA. The data are presented in Table 2 and include unpublished data for 3/16-in (4.76 mm) RHA (Bruchey 1997).

The values from Table 2 and an analytical fit to these data are plotted in Figure 3. A logarithmic form was chosen; the computed fit of the data is

$$y = (-0.1428)\ln t + 0.8772, \quad (4)$$

where y is the yield strength in GPa and t is the plate thickness in inches.

Table 2. Quasi-Static Yield Strength of RHA

Plate Thickness (in [mm])		Yield Strength (GPa)
0.1875	[4.76]	1.14
0.5	[12.7]	0.94
1.5	[38.1]	0.82
4.0	[101.6]	0.69

4. Fitting the Parameters

4.1 Parameter A. Parameter A is the yield strength at room temperature and a strain rate of 1/s. Equations (3a) through (3d) in Table 1 were interpolated to generate a function describing the behavior of the 2-in RHA at a strain rate of 1/s. The resulting function is

$$y = 1.5384\epsilon^{0.0436}. \quad (5)$$

A comparison of equations (5) and (3a) (Table 1) shows a difference of less than 2% between the yield strength at $\dot{\epsilon} = 1/s$ and $\dot{\epsilon} = 0.001/s$ at a strain of 0.01. Furthermore, Benck and Robitaille (1977) report a difference of about 1.1% for 38-mm RHA plate and about 0.6% for 100-mm

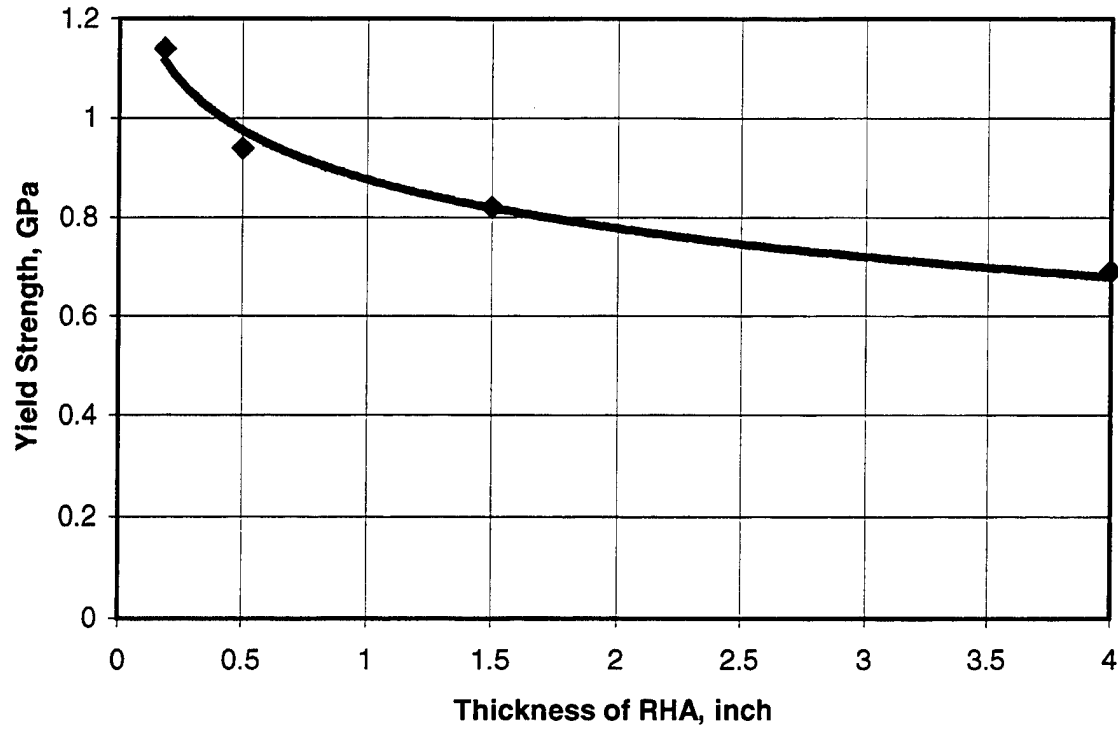


Figure 3. Quasi-Static Yield Strength of RHA.

RHA plate between the quasi-static yield strength at 0.0003/s and at 0.42/s. For the present work, the value of A is approximated by the quasi-static data (Table 2 and equation [4]). A value of $A = 0.78$ GPa for 2-in-thick RHA is obtained from equation (4).

4.2 Parameters B and n . The remaining parameters from equation (1) (B , C , m , and n) are fit to the functions of Table 1 by a least-squares technique. To fit the parameters B and n , write the first two terms of equation (1) as

$$Y = A \left(1 + \frac{B}{A} \epsilon^n \right). \quad (6)$$

Equation (6) represents the yield strength at room temperature and strain rate of 1/s, conditions that render the last two terms in equation (1) equal to unity. Equation (6) is rearranged to

$$Y - A = B\varepsilon^n. \quad (7)$$

Let

$$\varphi = \ln(Y - A) \quad (8)$$

so that

$$\varphi = n \ln \varepsilon + b, \quad (9)$$

where $b = \ln B$.

The data at these conditions are given by equation (5), which is of the form

$$y = \beta \varepsilon^\alpha. \quad (10)$$

The data must be in the same form as equation (8), so A is subtracted from both sides of equation (10), leading to the following representation of the data:

$$\Psi = \ln(y - A), \quad (11)$$

and

$$\Psi = \ln(\beta \varepsilon^\alpha - A). \quad (12)$$

The error incurred by approximating the data (equation [11]) with the model (equation [8]) at a strain ε_i is $\varphi_i - \Psi_i$. Subscript i represents an arbitrary discretization of the data into seven strains covering the range of the data ($\varepsilon = 0.01, 0.02, 0.04, 0.08, 0.12, 0.16$, and 0.20). This was done to simplify the fitting procedure. In the least-squares method, the error is squared (to avoid having positive and negative errors combining arithmetically to reduce the total error) and summed over the range of the data; the sum of the squared errors is to be minimized:

$$\sum_{i=1}^7 (\varphi_i - \Psi_i)^2 = \text{minimum.} \quad (13)$$

The sum can be minimized with respect to parameters B and n if the derivatives are set equal to zero. That is,

$$\frac{\partial}{\partial b} \sum_{i=1}^7 (\varphi_i - \Psi_i)^2 = 0, \quad (14)$$

and

$$\frac{\partial}{\partial n} \sum_{i=1}^7 (\varphi_i - \Psi_i)^2 = 0. \quad (15)$$

Equation (9) is substituted, and the differentiation is carried out, resulting in the following two equations:

$$b = \frac{\sum \Psi_i \ln \varepsilon_i \sum \ln \varepsilon_i - \sum \Psi_i \sum (\ln \varepsilon_i)^2}{(\sum \ln \varepsilon_i)^2 - 7 \sum (\ln \varepsilon_i)^2}, \quad (16)$$

and

$$n = \frac{\sum \Psi_i - 7b}{\sum \ln \varepsilon_i}, \quad (17)$$

where $\Psi_i = \Psi_i(\varepsilon_i)$ is known (equation [12]), and the summation indexes have been omitted for clarity. The results are $B = 0.78$ GPa and $n = 0.106$. These results minimize the error; this was verified by determining that the derivatives of equations (14) and (15) were positive.

4.3 Parameter C. The first two factors in equation (1) are

$$Y(\epsilon_i, \dot{\epsilon}^* = 1, T^* = 0) = A \left(1 + \frac{B}{A} \epsilon_i^n \right) = S_i, \quad (18)$$

where, for simplicity, this contribution to the strength is termed S_i . Thus, for room temperature, equation (1) becomes

$$Y_i = S_i (1 + C \ln \dot{\epsilon}^*) (1 - 0) = S_i + S_i C \ln \dot{\epsilon}^*. \quad (19)$$

To obtain a corresponding expression for the data, equations (3a) through (3d) (Table 1) are used to generate curves of stress vs. $\ln \dot{\epsilon}^*$ for various constant strains. To generate the curves, the first of the seven discrete strains was substituted into each of equations (3a) through (3d) (Table 1) to generate stresses for each of the four strain rates. The resulting stress was plotted against $\ln \dot{\epsilon}^*$, and the process repeated for each of the remaining six strains, resulting in seven curves. Analytical expressions were fit to the curves; the results are detailed in Table 3.

Table 3. Strain-Rate Dependence of Room-Temperature Data

i	Strain	$y = u_i + v_i \ln \dot{\epsilon}^*$		Equation No.
		u_i	v_i	
1	0.01	1.2587	0.0035	(20a)
2	0.02	1.2972	0.0039	(20b)
3	0.04	1.3370	0.0044	(20c)
4	0.08	1.3780	0.0050	(20d)
5	0.12	1.4026	0.0053	(20e)
6	0.16	1.4203	0.0055	(20f)
7	0.20	1.4342	0.0057	(20g)

(20)

These data can be represented by the form

$$y_i = s_i + s_i k_i \ln \dot{\epsilon}^*, \quad (21)$$

where the subscript i denotes each of the seven discrete strains in Table 3. Equations (19) and (21) are substituted into the least-squares function

$$\frac{\partial}{\partial C} \sum (Y_i - y_i)^2 = 0, \quad (22)$$

resulting in the following equation for C :

$$C = \frac{\sum s_i^2 k_i}{\sum s_i^2}. \quad (23)$$

This was verified to be a minimum by examining the derivative with respect to C of equation (22). The solution of equation (23), using all seven sets of constants in Table 3, is $C = 0.0035$. Using only the constants for $\varepsilon = 0.20$, an upper limit (limited by the extent of the data) of C for large strains is $C = 0.0040$. The lower limit (using only $\varepsilon = 0.01$ constants) is $C = 0.0028$.

4.4 Parameter m . Parameter m is determined by a technique based on a method described by Johnson and Cook (1983). Equation (1) is rewritten in the form

$$Y_T = Y_r (1 - T^{*m}), \quad (24)$$

where Y_T represents the strength at temperature T , and the room-temperature strength is

$$Y_r = A \left(1 + \frac{B}{A} \varepsilon^n \right) (1 + C \ln \dot{\varepsilon}^*). \quad (25)$$

The thermal-softening factor is obtained from equation (24):

$$\phi = \ln \left(1 - \frac{Y_T}{Y_r} \right), \quad (26)$$

so that, also

$$\phi = m \ln T^*. \quad (27)$$

Note that $\phi = \phi(\epsilon, \dot{\epsilon}, T^*)$, but strain rate will be held constant for this analysis. The data must be reduced to a similar form:

$$\Psi = \ln \left(1 - \frac{y_T}{y_r} \right). \quad (28)$$

Only data at a strain rate of 3,000/s were used for this analysis. Since the original data (Table 1) do not include room-temperature data at this strain rate, the available room temperature data (at strain rates of 0.001/s, 0.1/s, 3,500/s, and 7,000/s) were interpolated to obtain values of strength (y_r) at a strain rate of 3,000/s.

Data in the form y_T/y_r were plotted vs. T^* , and analytical fits were determined. Here, a good fit to the data was quadratic:

$$\frac{y_T}{y_r} = a_i T^{*2} + b_i T^* + c_i. \quad (29)$$

The results of the fitting are given in Table 4.

Reference data is available at 293 K (i.e., y_r). Elevated temperature data is available at 473 K and 673 K. Hence, the least squares optimization is fit for m at two known values of T^* , denoted by the subscript j .

Table 4. Quadratic Fit of the Temperature Data

i	Strain	$f(T^*) = y_T/y_r = a_i T^{*2} + b_i T^* + c_i$			Equation No.
		a_i	b_i	c_i	
1	0.01	-0.2436	-0.7662	1.0093	(30a)
2	0.02	-0.2030	-0.8029	1.0057	(30b)
3	0.04	-0.1627	-0.8394	1.0021	(30c)
4	0.08	-0.1229	-0.8755	0.9985	(30d)
5	0.12	-0.0998	-0.8965	0.9965	(30e)
6	0.16	-0.0835	-0.9114	0.9950	(30f)
7	0.20	-0.0708	-0.9228	0.9939	(30g)

(30)

To obtain a globally (i.e., over the range of temperatures) optimized value for m , the optimization formulation is

$$\sum_{j=1}^2 \sum_{i=1}^7 (\varphi_{ij} - \Psi_{ij})^2 = \text{minimum.} \quad (31)$$

Equation 27 is substituted, and the result is differentiated with respect to m and set equal to zero. This yields the following equation for m . The summation indices have been omitted for clarity, and $\Psi_{ij} = \Psi_{ij}(\varepsilon_i, T_j^*)$ is obtained from equations (28) to (30).

$$m = \frac{\sum \sum \Psi_{ij} \ln T^*}{\sum \sum (\ln T^*)^2}. \quad (32)$$

The result of this optimization over the range of strains is $m = 1.07$. Plots of the quadratic fits in Table 4 show that the curves approach a straight line as ε approaches a value slightly higher than 0.20 (i.e., slightly beyond the range of the data). Hence, for strains slightly greater than 0.20, $m = 1$. For small strains, equation (31) was solved for only the $\varepsilon = 0.01$ term ($i = 1$), with the result $m = 1.18$. A value of $m = 1.00$ was chosen for the present work (see section 5) in order to

favor the higher strains. This resulted in a variation of less than 1% in depth of penetration when compared to a similar simulation using a value of $m = 1.07$.

5. Numerical Simulations

The continuum mechanics code CTH was used to run a series of three-dimensional (3-D) computations simulating experimental ballistic impacts. These simulations were run in order to validate the aforementioned method for determining Johnson-Cook fit parameters for RHA. All computations were conducted on a Cray J932 computer at ARL's Major Shared Resource Center (MSRC).

5.1 Setup. The simulations were modeled after experiments that were performed by Enderlein (1991) in which 20-mm-diameter by 100-mm-long ($l/d = 5$) X21C tungsten alloy rods (right circular cylinders) were fired into stacks of four 2.5-in-thick (63.5-mm) RHA plates at 0° obliquity. These experiments were chosen as model candidates because the 2.5-in-thick RHA plates that were used closely resembled the 2-in (51-mm) RHA for which dynamic strength data were available, to the extent that they are in the same thickness group in MIL-A-12560H (Figure 1). Penetrator impact velocities used in the simulation matrix corresponded to measured experimental striking velocities of 1,399 m/s and 1,616 m/s.

Figure 4 shows the setup that was used for each simulation. Each problem was modeled in three dimensions. The penetrator was inserted as a right circular cylinder with dimensions that matched the experiment. Eleven Lagrangian tracers were placed along its centerline to monitor several variables, including depth of penetration. The penetrator was fired in the x direction at the stack of RHA plates. The 2.5-in RHA plates were inserted with a 0.5-mm gap between each other to ensure (numerically) the existence of an interface. The lateral dimensions of the RHA plates were chosen to be 8 in \times 8 in (203 mm \times 203 mm) in the simulations. Symmetry was used about the XZ plane in order to reduce problem size. A constant cell size of 2 mm was selected to finely resolve each problem, and this resulted in a volume of approximately one million cells per problem.

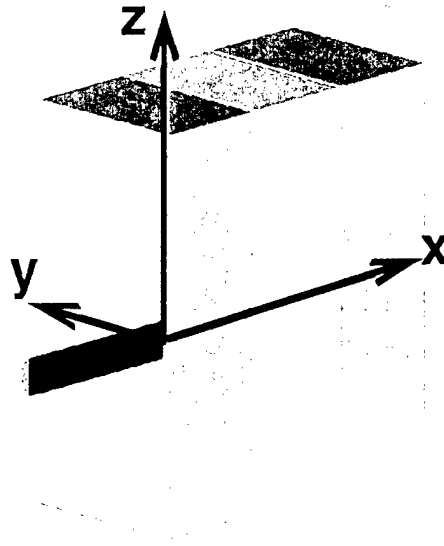


Figure 4. Simulation Setup.

The Mie-Grüniesen equation of state and the Johnson-Cook strength model were used for all materials. Default Johnson-Cook parameters were taken for the penetrator in each simulation. These parameters are given by Johnson and Cook (1983) for 90% tungsten alloy. Johnson-Cook parameters were then varied for the RHA in each run.

Six simulations were run for each of the two different striking velocities. Each simulation set corresponds to a particular group of Johnson-Cook parameters, as shown in Table 5. Set 1 contains the default parameters given in CTH. They are one of the sets derived in Gray et al. (1994). A nondimensional temperature definition different from that of equation (2) was used by Gray et al. (1994), so using these parameters in CTH may not be optimum. Set 2 is the set of parameters derived above for 2-in RHA. Sets 3 through 6 are variations included for information and lend support to the validity of Set 2 for 2-in RHA. These sets are discussed in the following sections.

5.2 Results. Table 6 compares the measured penetrations for the experiment and the six sets of simulations. The experimental data consist of a single shot at each velocity. The depth of penetration for each simulation was determined by using the tracer at the nose of the penetrator.

Table 5. RHA Parameter Sets Evaluated

Parameter	Set 1 ^a	Set 2 ^b	Set 3 ^c	Set 4 ^d	Set 5 ^e	Set 6 ^f
A (GPa)	1.832	0.78	0.74	1.225	0.9	0.78
B (GPa)	1.685	0.78	0.78	1.575	1.305	0.78
n	0.754	0.106	0.106	0.768	0.90	0.106
C	0.00435	0.004	0.004	0.0049	0.0575	0.0891
m	0.80	1.00	1.00	1.09	1.075	1.00

^a CTH default.^b 2-in RHA (recommended parameters for 2-in RHA).^c 2.5-in RHA (estimated).^d Fit from Gray et al. (1994) using all strain rate data.^e Fit from Gray et al. (1994) using only high strain rate data.^f Current fitting technique using only high strain rate data to fit C.**Table 6. RHA Penetrations in Millimeters for the Parameter Sets Evaluated**

Velocity	Experiment	Set 1	Set 2	Set 3	Set 4	Set 5	Set 6
1,399 m/s	101	72	97	99	85	85	71
1,616 m/s	133	91	117	119	105	104	88

This is illustrated in Figure 5, which shows a time history of the x position of the nose and tail tracers for the 1,616-m/s 2-in RHA run.

Set 1 in Table 6 shows that the default Johnson-Cook RHA parameters in CTH lead to underprediction of the depth of penetration for these experiments. In fact, the penetration is underpredicted by more than 28% for both velocities. There is a significant improvement in the penetration results when the parameters for the fit to the 2-in dynamic data are used (Set 2 of Table 6). The penetrations increase to within 4% of experiment for the 1,399-m/s case and to within 12% of experiment for the 1,616-m/s case.

The underprediction of penetration depth when using the parameters for the 2-in RHA was expected because the experiment used the softer 2.5-in RHA (see Figure 3). Had the parameters for 2.5-in RHA been available, the simulation with these parameters may have shown

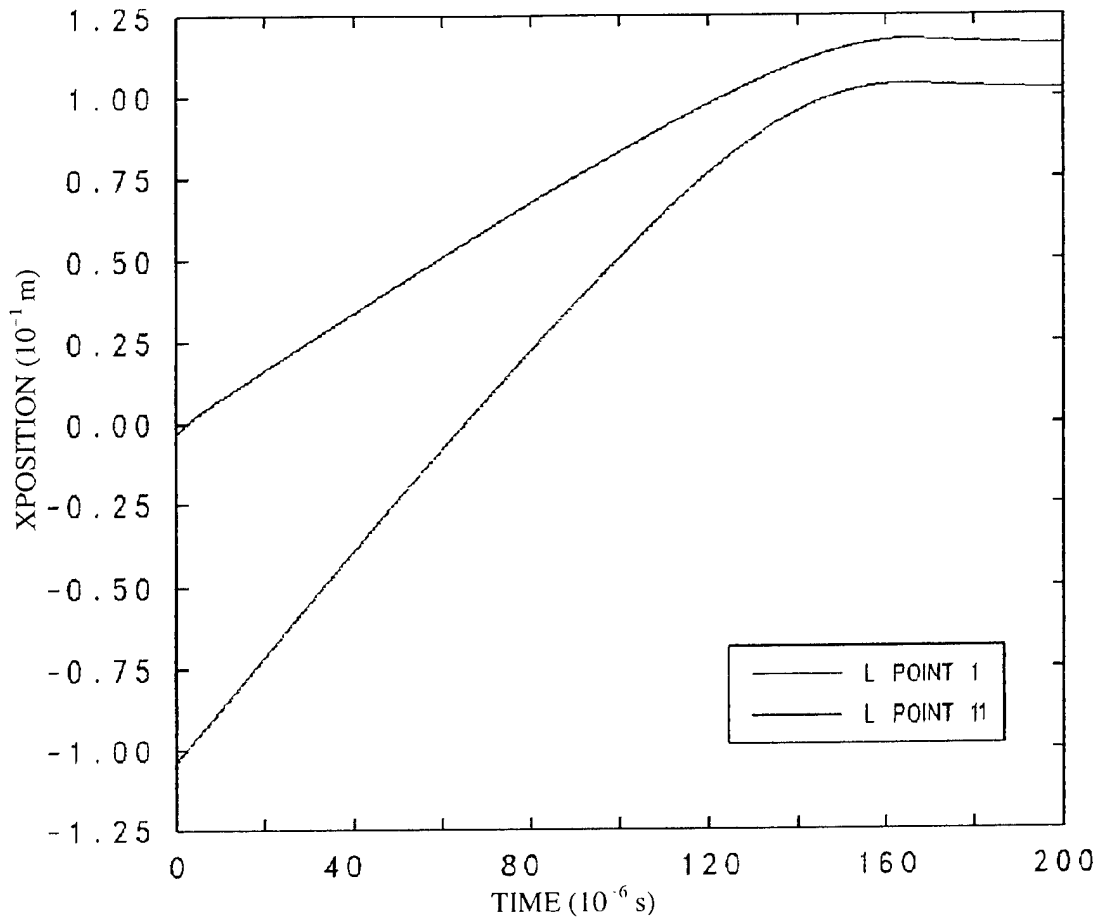


Figure 5. Nose and Tail Tracer Histories for the 1,616 m/s, Set 2 Case.

penetrations even closer to experiment. To demonstrate this, the A parameter was changed to 0.74 GPa to approximate the quasi-static yield strength of 2.5-in RHA. As expected, the results from this simulation (Set 3) show a slight improvement in predicted penetration for both velocities. For future analysis, dynamic data should be obtained for 2.5-in RHA, fit using the aforementioned method, and modeled in CTH.

Set 4 of Table 6 shows the result of using the Gray et al. (1994) fit for 2-in-thick RHA that considers the same temperature function as CTH, that of equation (2). This set of parameters predicts penetration into semi-infinite RHA better than when using the CTH default set (Set 1), but not as well as when using the parameter set derived here (Set 2). Sets 5 and 6 are discussed in the next section.

5.3 Discussion. The extent of the experimental variation may be inferred from three shots fired by Enderlein (1991) into stacks of 2.5-in RHA at 30° obliquity. The velocities of these shots were nominally 1,606 m/s (± 2 m/s), and penetrations varied by 9%. In addition, a 30° oblique shot at 1,652 m/s penetrated 132 mm, indicating that the data in Table 6 for the high-velocity case may be above average. This experimental variation may reduce the discrepancy between the predicted and experimental values in Table 6 for the high-velocity case.

Several factors other than RHA strength will affect depth of penetration. One possible explanation for the slightly low CTH predictions is that the model for the penetrator does not precisely mimic the X21C (93%) tungsten alloy used in the experiments. The validity of the model was not tested here; it is a widely used model and was chosen to facilitate comparisons to other work.

Another possibility is that the simulated interfaces between the plates do not accurately imitate the experimental ones (for one reason, they are made up of mixed cells). This may be a more important factor for the high-velocity cases because the penetrators get further into the second plate and the model must contend with a second interface (Figure 6).

Hardness of RHA (and therefore strength) is known to vary through the thickness of the plate, especially for the thicker stock. Since the RHA was modeled as homogeneous for a given thickness, this inhomogeneity could lead to differences between the experiments and the simulations.

Failure (of both the RHA and tungsten) was modeled with a basic threshold fracture model only (the “pfrac” parameter in CTH). This parameter is typically chosen as the spall strength of the material (2.5 GPa for RHA and 3.0 GPa for tungsten). This model was kept constant during this study in order to simplify interpretation of results. No other damage or fracture models were used. However, fracture and damage are important in ballistic problems, as shown, for example, by Raftenberg (1997a). This area warrants further study.

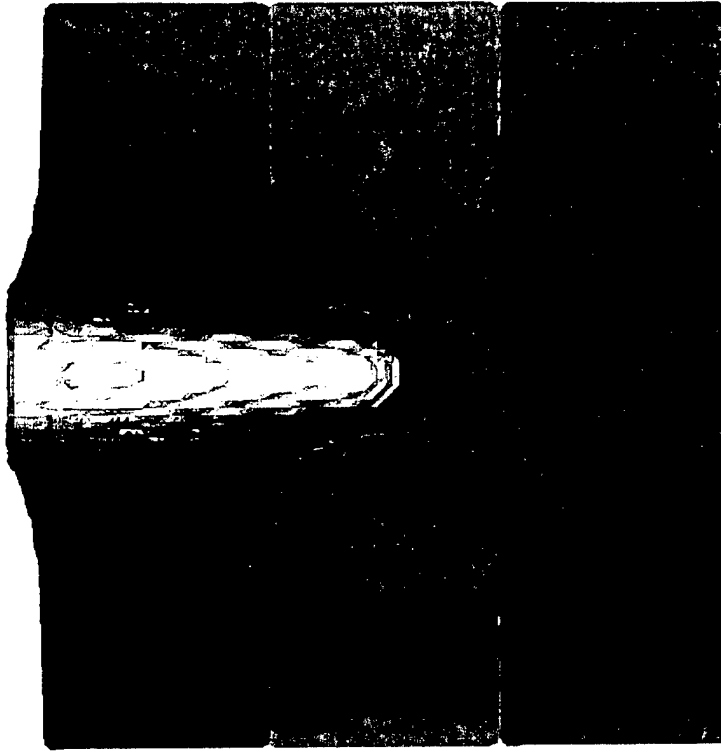


Figure 6. Set 2: 1,616-m/s Penetration Plot.

CTH plots showed that the strain rate at the penetration interface is as high as $10^5/s$ at initial impact and sustains values on the order of $10^4/s$ during steady-state penetration. Raftenberg (1997b) pointed out that the Johnson-Cook form of strain-rate dependence may not fit the response of RHA well for this problem; C may deviate from constant at strain-rates greater than $10^3/s$. This is indeed the case with the dynamic data studied here (Table 1). In order to investigate the effect of this deviation, two additional simulation sets were conducted (Sets 5 and 6 in Tables 5 and 6). Set 5 uses the Gray et al. (1994) fit of only the high strain-rate data. The result was virtually unchanged from Set 4, with the Gray et al. (1994) fit using all of the data. A similar attempt was made here, wherein the parameter C was fit using only the high strain-rate data (3,500/s and 7,000/s); a value of 0.0891 resulted. All other parameters were unchanged from Set 2. The resulting penetration depths at both velocities were severely underpredicted. This underprediction is not surprising, since making such a change to C , which is a *constant*, will strengthen the RHA at all strain rates throughout the block. The least-squares method used for the strength data in Table 5 (Set 2) selected an optimum value for C over the full range of strain

rates. This should provide a reasonable value for a variety of applications, but further study of C is warranted.

6. Conclusion

A method for fitting static and dynamic strength data for RHA in order to obtain parameters for the Johnson-Cook constitutive model has been presented. This method can be used to obtain parameters for available thicknesses of RHA, provided dynamic data exist. Parameters were obtained from 2-in RHA data, tested using CTH, and shown to significantly improve predictions for a particular set of experimental data when compared to predictions obtained using two sets of previously published parameters, including the CTH default set.

INTENTIONALLY LEFT BLANK.

7. References

- Benck, R. F. "Quasi-Static Tensile Stress Strain Curves—II, Rolled Homogeneous Armor." BRL-MR-2703, U.S. Army Ballistic Research Laboratory, Aberdeen Proving Ground, MD, 1976.
- Benck, R. F., and J. L. Robitaille. "Tensile Stress-Strain Curves—III, Rolled Homogeneous Armor at a Strain Rate of 0.42s^{-1} ." BRL-MR-2760, U.S. Army Ballistic Research Laboratory, Aberdeen Proving Ground, MD, 1977.
- Bruchey, W. J. Personal communication. U.S. Army Research Laboratory, Aberdeen Proving Ground, MD, 1997.
- Enderlein, M. W. "Armor Backpack Effectiveness Against Rod Penetrators at Ordnance Velocities." BRL-MR-3939, U.S. Army Ballistic Research Laboratory, Aberdeen Proving Ground, MD, 1991.
- Gray, G. T., S. R. Chen, W. Wright, and M. F. Lopez. "Constitutive Equations for Annealed Metals Under Compression at High Strain Rates and High Temperatures." LA-12669-MS, Los Alamos National Laboratory, NM, 1994.
- Johnson, G. R., and W. H. Cook. "A Constitutive Model and Data for Metals Subjected to Large Strains, High Strain Rates and High Temperatures." *Proceedings of the Seventh International Symposium on Ballistics*, pp. 541–547, The Hague, Netherlands, 1983.
- McGlaun, J. M., S. L. Thompson, and M. G. Elrick. "CTH: A Three-Dimensional Shock Wave Physics Code." *International Journal of Impact Engineering*, vol. 10, pp. 351–360, 1990.
- Raftenberg, M. N. "Tensile Damage Effects in Steel Plate Perforation by a Tungsten Rod." *Proceedings of the 1997 APS Conference on Shock Compression of Condensed Matter*, S. C. Schmidt (editor), American Physical Society, 1997a.
- Raftenberg, M. N. "Close-In Blast Loading of a Steel Disc; Sensitivity to Steel Strength Modeling." *International Journal of Impact Engineering*, vol. 20, pp. 651–662, 1997b.
- U.S. Department of Defense. *Military Specification: Armor Plate, Steel, Wrought, Homogeneous (for Use in Combat Vehicles and for Ammunition Testing)*. MIL-A-12560H, Washington, DC, 1991.

INTENTIONALLY LEFT BLANK.

<u>NO. OF COPIES</u>	<u>ORGANIZATION</u>
2	DEFENSE TECHNICAL INFORMATION CENTER DTIC OCA 8725 JOHN J KINGMAN RD STE 0944 FT BELVOIR VA 22060-6218
1	HQDA DAMO FDT 400 ARMY PENTAGON WASHINGTON DC 20310-0460
1	OSD OUSD(A&T)/ODDR&E(R) DR R J TREW 3800 DEFENSE PENTAGON WASHINGTON DC 20301-3800
1	COMMANDING GENERAL US ARMY MATERIEL CMD AMCRDA TF 5001 EISENHOWER AVE ALEXANDRIA VA 22333-0001
1	INST FOR ADVNCD TCHNLGY THE UNIV OF TEXAS AT AUSTIN 3925 W BRAKER LN STE 400 AUSTIN TX 78759-5316
1	DARPA SPECIAL PROJECTS OFFICE J CARLINI 3701 N FAIRFAX DR ARLINGTON VA 22203-1714
1	US MILITARY ACADEMY MATH SCI CTR EXCELLENCE MADN MATH MAJ HUBER THAYER HALL WEST POINT NY 10996-1786
1	DIRECTOR US ARMY RESEARCH LAB AMSRL D DR D SMITH 2800 POWDER MILL RD ADELPHI MD 20783-1197

<u>NO. OF COPIES</u>	<u>ORGANIZATION</u>
1	DIRECTOR US ARMY RESEARCH LAB AMSRL CI AI R 2800 POWDER MILL RD ADELPHI MD 20783-1197
3	DIRECTOR US ARMY RESEARCH LAB AMSRL CI LL 2800 POWDER MILL RD ADELPHI MD 20783-1197
3	DIRECTOR US ARMY RESEARCH LAB AMSRL CI IS T 2800 POWDER MILL RD ADELPHI MD 20783-1197
	<u>ABERDEEN PROVING GROUND</u>
2	DIR USARL AMSRL CI LP (BLDG 305)

<u>NO. OF COPIES</u>	<u>ORGANIZATION</u>
2	SANDIA NATIONAL LAB E S HERTEL P A TAYLOR MS 0819 PO BOX 5800 ALBUQUERQUE NM 87185-0819
2	SOUTHWEST RESEARCH INST ENGR DYNAMICS DEPT C ANDERSON J WALKER PO BOX DRAWER 28510 SAN ANTONIO TX 78228
3	INST FOR ADVNCD TCHNLGY THE UNIV OF TEXAS AT AUSTIN S BLESS D LITTLEFIELD D GEE 3925 W BRAKER LN STE 400 AUSTIN TX 78759-5316
1	JOHNS HOPKINS UNIVERSITY DEPT MECH ENGRG K RAMESH CHARLES AND 33 ST BALTIMORE MD 21218
1	BROWN UNIVERSITY DIV OF ENGRG R CLIFTON PROVIDENCE RI 02912
1	ARMY RESEARCH OFFICE AMSRL RO EN A RAJENDRAN DURHAM NC 27709-2211
1	UNIVERSITY OF CALIFORNIA AT SAN DIEGO DEPT APPLIED MECH & ENGRG SCIENCES S NEMAT-NASSER LA JOLLA CA 92093-0416
1	NORTHWESTERN UNIVERSITY DEPT MECH ENGRG H ESPINOSA EVANSTON IL 60208-3111

<u>NO. OF COPIES</u>	<u>ORGANIZATION</u>
	<u>ABERDEEN PROVING GROUND</u>
36	DIR USARL AMSRL WM MC M STAKER J BEATTY AMSRL WM TA W BRUCHEY H MEYER (3 CPS) D KLEPONIS (3 CPS) P KINGMAN Y HUANG A MIHALCIN M ZOLTOSKI T HAVEL M NORMANDIA E HORWATH P BARTOWSKI M KEELE R LEAVY M BURKINS J RUNYEON D MACKENZIE AMSRL WM TB R FREY W LAWRENCE J STARKENBERG AMSRL WM TC R COATES K KIMSEY D SHEFFLER S SHRAML R SUMMERS AMSRL WM TD D GROVE M RAFTENBERG S SEGLETES S SCHOENFELD E RAPACKI AMSRL WM TE A NIILER

REPORT DOCUMENTATION PAGE			Form Approved OMB No. 0704-0188	
Public reporting burden for this collection of information is estimated to average 1 hour per response, including the time for reviewing instructions, searching existing data sources, gathering and maintaining the data needed, and completing and reviewing the collection of information. Send comments regarding this burden estimate or any other aspect of this collection of information, including suggestions for reducing this burden, to Washington Headquarters Services, Directorate for Information Operations and Reports, 1215 Jefferson Davis Highway, Suite 1204, Arlington, VA 22202-4302, and to the Office of Management and Budget, Paperwork Reduction Project (0704-0188), Washington, DC 20503.				
1. AGENCY USE ONLY (Leave blank)		2. REPORT DATE June 2001	3. REPORT TYPE AND DATES COVERED Final, January 1998–March 1998	
4. TITLE AND SUBTITLE An Analysis of Parameters for the Johnson-Cook Strength Model for 2-in-Thick Rolled Homogeneous Armor			5. FUNDING NUMBERS AH80	
6. AUTHOR(S) Hubert W. Meyer, Jr. and David S. Kleponis				
7. PERFORMING ORGANIZATION NAME(S) AND ADDRESS(ES) U.S. Army Research Laboratory ATTN: AMSRL-WM-TA Aberdeen Proving Ground, MD 21005-5066			8. PERFORMING ORGANIZATION REPORT NUMBER ARL-TR-2528	
9. SPONSORING/MONITORING AGENCY NAMES(S) AND ADDRESS(ES)			10. SPONSORING/MONITORING AGENCY REPORT NUMBER	
11. SUPPLEMENTARY NOTES				
12a. DISTRIBUTION/AVAILABILITY STATEMENT Approved for public release; distribution is unlimited.			12b. DISTRIBUTION CODE	
13. ABSTRACT (Maximum 200 words) Yield strength obtained from quasi-static strength data for rolled homogeneous armor (RHA) was combined with dynamic strength data for 2-in (51-mm) RHA to generate Johnson-Cook parameters for 2-in RHA. One parameter was fixed based on the quasi-static strength data, and a least-squares method was used to fit the others individually. The fit was tested with CTH by simulating the penetration of stacks of 2.5-in-thick (63.5-mm) RHA plates (the closest available experimental data). Parameter analysis and comparison of the simulations to experiment substantiated the approach.				
14. SUBJECT TERMS penetration, yield strength, RHA, armor, CTH			15. NUMBER OF PAGES 28	
			16. PRICE CODE	
17. SECURITY CLASSIFICATION OF REPORT UNCLASSIFIED	18. SECURITY CLASSIFICATION OF THIS PAGE UNCLASSIFIED	19. SECURITY CLASSIFICATION OF ABSTRACT UNCLASSIFIED	20. LIMITATION OF ABSTRACT UL	

INTENTIONALLY LEFT BLANK.

USER EVALUATION SHEET/CHANGE OF ADDRESS

This Laboratory undertakes a continuing effort to improve the quality of the reports it publishes. Your comments/answers to the items/questions below will aid us in our efforts.

1. ARL Report Number/Author ARL-TR-2528 (Meyer) Date of Report June 2001
2. Date Report Received _____
3. Does this report satisfy a need? (Comment on purpose, related project, or other area of interest for which the report will be used.) _____

4. Specifically, how is the report being used? (Information source, design data, procedure, source of ideas, etc.) _____

5. Has the information in this report led to any quantitative savings as far as man-hours or dollars saved, operating costs avoided, or efficiencies achieved, etc? If so, please elaborate. _____

6. General Comments. What do you think should be changed to improve future reports? (Indicate changes to organization, technical content, format, etc.) _____

CURRENT
ADDRESS

Organization

Name

E-mail Name

Street or P.O. Box No.

City, State, Zip Code

7. If indicating a Change of Address or Address Correction, please provide the Current or Correct address above and the Old or Incorrect address below.

OLD
ADDRESS

Organization

Name

Street or P.O. Box No.

City, State, Zip Code

(Remove this sheet, fold as indicated, tape closed, and mail.)
(DO NOT STAPLE)

DEPARTMENT OF THE ARMY

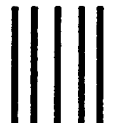
OFFICIAL BUSINESS

BUSINESS REPLY MAIL

FIRST CLASS PERMIT NO 0001,APG,MD

POSTAGE WILL BE PAID BY ADDRESSEE

DIRECTOR
US ARMY RESEARCH LABORATORY
ATTN AMSRL WM TA
ABERDEEN PROVING GROUND MD 21005-5066



NO POSTAGE
NECESSARY
IF MAILED
IN THE
UNITED STATES

